Thirst recruits phasic dopamine signaling through subfornical organ neurons

Ted M. Hsu[a], Paula Bazzino[a,b], Samantha J. Hurh[a], Vaibhav R. Konanur[a,b], Jamie D. Roitman[a,b], and Mitchell F. Roitman[a,b,1]

[a]Department of Psychology, University of Illinois at Chicago, Chicago, IL 60607; and [b]Graduate Program in Neuroscience, University of Illinois at Chicago, Chicago, IL 60607

Edited by Richard D. Palmiter, University of Washington School of Medicine, Seattle, WA, and approved October 8, 2020 (received for review May 8, 2020)

Thirst is a highly potent drive that motivates organisms to seek out and consume balance-restoring stimuli. The detection of dehydration is well understood and involves signals of peripheral origin and the sampling of internal milieu by first order homeostatic neurons within the lamina terminalis—particularly glutamatergic neurons of the subfornical organ expressing CaMKIIa (SFO^{CaMKIIa}). However, it remains unknown whether mesolimbic dopamine pathways that are critical for motivation and reinforcement integrate information from these "early" dehydration signals. We used in vivo fiber photometry in the ventral tegmental area and measured phasic dopamine responses to a water-predictive cue. Thirst, but not hunger, potentiated the phasic dopamine response to the water cue. In euvolemic rats, the dipsogenic hormone angiotensin II, but not the orexigenic hormone ghrelin, potentiated the dopamine response similarly to that observed in water-deprived rats. Chemogenetic manipulations of SFO^{CaMKIIa} revealed bidirectional control of phasic dopamine signaling during cued water reward. Taking advantage of within-subject designs, we found predictive relationships between changes in cue-evoked dopamine response and changes in behavioral responses—supporting a role for dopamine in motivation induced by homeostatic need. Collectively, we reveal a putative mechanism for the invigoration of goal-directed behavior: internal milieu communicates to first order, need state-selective circuits to potentiate the mesolimbic dopamine system's response to cues predictive of restorative stimuli.

homeostasis | motivation | reward | fiber photometry | ventral tegmental area

The invigoration of goal-directed behaviors is fundamentally grounded in homeostatic need. The maintenance of body fluid is a robust demonstration of the homeostasis-to-action arc, where minute changes can alter an animal's motivation to seek and consume previously neutral (e.g., water) or even aversive (e.g., salt) stimuli (see refs. 1 and 2 for review). Plasma volume and osmolality are monitored through multiple mechanisms. For example, specialized cells of the kidney sense decreases in plasma perfusion and initiate the renin–angiotensin cascade resulting in the elevation of the hormone angiotensin II (AngII)—which acts in the central nervous system to increase water and sodium consumption (3–5). Circumventricular organs, particularly the lamina terminalis (i.e., subfornical organ [SFO], organum vasculosum [OVLT], and median preoptic nucleus [MnPO]), are thought to be central first order detectors of changes in body fluid composition (2, 6) and respond to AngII (7, 8). A series of elegant studies have shown that activation of specific populations of SFO neurons are sufficient to drive water consumption even in euvolemia (i.e., normal body fluid balance) (9, 10). These same SFO neurons increase their activity in response to dehydration and their activity is reduced when thirsty animals begin drinking (11).

While the SFO detects body fluid imbalance, it must relay this information to marshal motive circuits for seeking and consuming fluid in response to need. Indeed, thirst recruits widespread networks across the brain, including those involved in motivation (12). Phasic activity of midbrain dopamine neurons in the ventral tegmental area (VTA) and dopamine release in the nucleus accumbens (NAc) play critical roles in motivation. Phasic dopamine responses are linked to stimulus valence (13–17), salience (18–22), reinforcement (23), and goal-directed action (24, 25) with recent work suggesting that their roles in these psychological constructs are not mutually exclusive (26). Perturbations in homeostasis tune dopamine responses. For example, hunger powerfully augments phasic dopamine responses to cues that predict food (27–29)—an effect recapitulated by central delivery of gut hormones that regulate hunger and satiety (28, 30). Changes in body fluid homeostasis [dehydration (31) or sodium depletion (32)] generate state-specific phasic dopamine responses to the intraoral delivery of fluid balance-restoring stimuli (water or hypertonic saline) or their predictive cues. How information about fluid balance reaches dopamine neurons remains unclear.

Circumventricular organs, with their fenestrated blood–brain barrier, represent a potentially efficient way of communicating signals of peripheral origin that relate physiological need to central motive circuits. However, it remains unknown if and how central first order homeostatic neurons can modulate phasic dopamine signaling in the service of motivation. Understanding how homeostasis is communicated to the mesolimbic system is crucial for understanding the development of the enhanced cue reactivity that can underlie excessive ingestive behaviors. We trained rats to expect brief access to water in response to a cue and recorded either activity from VTA dopamine neurons or NAc dopamine release using fiber photometry. Thirst, but not hunger, potentiated dopamine responses to the water-predictive

Significance

The maintenance of body fluid homeostasis is critical for survival and very subtle deviations from fluid balance can prompt corrective action. These minute changes are detected by first order homeostatic neurons within circumventricular organs of the lamina terminalis but must be passed along to circuitry for motivated behavior. Water-predictive cues evoke robust increases in dopamine signaling in thirsty rats. We demonstrate that this cue-evoked phasic dopamine response is gated by body fluid status, the dipsogenic hormone angiotensin II, and select neurons of the subfornical organ. These data provide critical insight into the conversion of homeostatic imbalance into invigorated action.

Author contributions: T.M.H. and M.F.R. designed research; T.M.H., P.B., S.J.H., and V.R.K. performed research; T.M.H., V.R.K., J.D.R., and M.F.R. analyzed data; and T.M.H., J.D.R., and M.F.R. wrote the paper.

The authors declare no competing interest.

This article is a PNAS Direct Submission.

[1]To whom correspondence may be addressed. Email: mroitman@uic.edu.

This article contains supporting information online at https://www.pnas.org/lookup/suppl/doi:10.1073/pnas.2009233117/-/DCSupplemental.

First published November 16, 2020.

cue. Central delivery of AngII and modulation of excitatory SFO neurons using designer receptors exclusively activated by designer drug (DREADDs) recapitulated the effects of thirst. Collectively, the data support an intimate relationship between first order detectors of homeostatic imbalance and a system critical for converting motivation to action.

Results

In Vivo Fiber Photometry in the Mesolimbic Dopamine System Captures Water-Cue-Evoked Activity. To record dynamic activity of the mesolimbic dopamine system, we expressed fluorescent sensors and performed in vivo fiber photometry in the VTA and NAc (33, 34). Cre-dependent GCaMP6f (AAV1.Syn.Flex.GCaMP6f), to sense changes in intracellular calcium, was delivered to the VTA of TH:Cre^{+} rats and a fiber optic was chronically implanted at the injection site (see fiber optic placement for all experiments in *SI Appendix*, Fig. S1*A*). Consistent with our and other work (26, 30), this protocol permits selective expression of the construct in dopamine neurons (Fig. 1 *A*–*F*). We found good penetrance (36.1 ± 7.67% of tyrosine hydroxylase (TH)-positive neurons expressing GCaMP6f) and excellent selectivity (99.4 ± 0.62% of GCaMP6f-positive neurons coexpressed TH) of the viral construct (Fig. 1*G*; 10 sections/rat; No. of TH cells = 107.73 ± 7.57/section; No. of GFP cells = 41.3 ± 3.20/section). In a separate group of wild-type rats, we transfected the NAc dorsomedial shell with the fluorescent dopamine sensor dLight1.2 (*SI Appendix*, Fig. S1 *B*–*D*).

Dopamine neurons can exhibit phasic responses—particularly with respect to reward versus aversion—that can vary based on anatomical location and projection target (35–38). We characterized the responses of dopamine neurons in the targeted region of the VTA to intraoral infusions of taste stimuli and found that rewarding sucrose increased and aversive quinine decreased activity [Fig. 1*H*; $n = 5$; sucrose: $F(2, 8) = 30.31$, $P = 0.0002$; baseline (preinfusion) vs. infusion, $P = 0.0001$; quinine: $F(2, 8) = 26.82$, $P = 0.0004$; baseline (preinfusion) vs. infusion, $P = 0.0062$; *SI Appendix*, Table S1]—consistent with previous work recording phasic dopamine release in the NAc dorsomedial shell (14). Next, we determined that, in thirsty rats, phasic dopamine signals developed to cues predictive of water availability—consistent with extensive literature demonstrating time locking to cues associated with reward (24, 39–43). Rats ($n = 5$) were conditioned to anticipate the presentation of a retractable water sipper based on an audio cue (Fig. 1*I*). Rats quickly learned the cue–reward relationship (Fig. 1*J*, representative rat licking behavior by trial), evidenced by shorter latencies to the first lick following sipper presentation [Fig. 1 *K*, *Left*; $F(2, 8) = 74.65$; main effect of day $P < 0.0001$; day 1 vs. day 2, day 1 vs. day 3 $P < 0.0001$; day 2 vs. day 3 $P = 0.4071$] and increased lick rate during the first bout of licking [Fig. 1 *K*, *Right*; $F(2, 8) = 14.87$; main effect of day, $P = 0.0020$; day 1 vs. day 2 $P = 0.0137$; day 1 vs. day 3 $P = 0.0019$; day 2 vs. day 3 $P = 0.3228$]. Importantly, the acquisition of this behavior is reflected in phasic VTA dopamine neuron activity (Fig. 1*L*, average signal from all rats time locked to cue presentation across trials; Fig. 1*M*, single trial trace with licks), where the dopamine response evoked by the water-predictive cue increased across conditioning days [Fig. 1*N*, quantification in the *Inset*; $F(2, 8) = 8.688$; main effect of day $P = 0.0099$; day 1 vs. day 2 $P = 0.1244$; day 1 vs. day 3 $P = 0.0078$; day 2 vs. day 3 $P = 0.1925$]. While VTA dopamine neurons also respond to the first lick after sipper extension, responses across days were not significantly different [*SI Appendix*, Fig. S2*A*, $F(2, 8) = 0.2130$, $P = 0.8126$].

Phasic Dopamine Responses to a Water-Predictive Cue Are Selective for Physiological State. Need states are powerful drivers of goal-directed behaviors. We found that, after training under water restriction, hydration status modulated the phasic dopamine response to the water-predictive cue. Trained rats ($n = 8$) were given 2 d of ad libitum access to water. Then, in a counterbalanced, within-subjects design, rats either remained euvolemic or were overnight water deprived (2 d of ad libitum access between treatments). In water-deprived rats, the water-predictive cue evoked a robust increase in VTA dopamine neuron activity, a response that was significantly weaker when the same rats were tested euvolemic [Fig. 2*A*; quantification in Fig. 2*B*, $t(7) = 4.995$, $P = 0.0016$]. A similar effect was seen when dopamine activity is aligned to the first lick [*SI Appendix*, Fig. S2*B*; $t(7) = 3.524$, $P = 0.0097$]. In a separate cohort of rats ($n = 6$), hydration status had no impact on a nonpredictive cue [dopamine activity: *SI Appendix*, Fig. S3*A*; $t(5) = 1.556$, $P = 0.1804$; behavior: *SI Appendix*, Fig. S3*B* and Table S1]. Using the fluorescent dopamine sensor dLight1.2 to capture dopamine release in the NAc dorsomedial shell ($n = 7$), hydration status modulated dopamine release evoked by the water-predictive cue [Fig. 2*D*; quantification in Fig. 2*E*, $t(6) = 4.011$, $P = 0.0070$] but not for the first lick [*SI Appendix*, Fig. S2*C*, $t(6) = 1.336$, $P = 0.2300$]. Phasic dopamine responses encode reward-prediction error but also participate in learned behavioral responses to reward-predictive stimuli (25, 44). Importantly, we show that robust cue-evoked phasic dopamine responses are accompanied by increased behavioral responses for water reward (Figs. 1*M* and Fig. 2 *C* and *F*). When thirsty, rats exhibit significantly shorter latencies to approach the sipper relative to the euvolemic state [Fig. 2 *C*, *Left*: $t(7) = 3.823$, $P = 0.0065$; Fig. 2 *F*, *Left*: $t(6) = 9.842$, $P < 0.0001$; *SI Appendix*, Table S1] and faster lick rate in the first bout of licking [Fig. 2 *C*, *Right*: $t(7) = 4.553$, $P = 0.0026$; Fig. 2 *F*, *Right*: $t(6) = 7.072$, $P = 0.0004$; *SI Appendix*, Table S1]. To determine if other need states could modulate the dopamine response to the water-predictive cue, a separate cohort of rats ($n = 7$) was conditioned while water restricted. After conditioning and ad libitum access to water, overnight water deprivation (water dep) potentiated the dopamine response, relative to the euvolemic state. In contrast, overnight food deprivation failed to potentiate the dopamine response [order of state manipulations counterbalanced across rats; Fig. 2*G*; quantification in Fig. 2*H*, $F(2, 12) = 9.653$, $P = 0.0032$; euvolemic vs. food dep, $P = 0.3536$; euvolemic vs. water dep, $P = 0.0027$; water dep vs. food dep, $P = 0.0345$] and modulate behavioral responses for water [latency: Fig. 2 *I*, *Left*: $F(2, 12) = 11.09$, $P = 0.0019$, euvolemic vs. food dep, $P = 0.8645$; euvolemic vs. water dep, $P = 0.0067$; water dep vs. food dep, $P = 0.0027$; lick rate in the first bout: Fig. 2 *I*, *Right*: $F(2, 12) = 6.940$, $P = 0.0099$, euvolemic vs. food dep, $P = 0.5533$; euvolemic vs. water dep, $P = 0.0205$; water dep vs. food dep, $P = 0.0031$; *SI Appendix*, Table S1]. Similar selective modulation for dopamine activity aligned to first lick was also observed [*SI Appendix*, Fig. S2*D*; $F(2, 12) = 4.120$, $P = 0.0434$; euvolemic vs. food dep, $P = 0.06114$; euvolemic vs. water dep, $P = 0.0379$; water dep vs. food dep, $P = 0.1930$].

Collectively, specific need states selectively recruited phasic VTA dopamine responses to cues predictive of restorative stimuli. The strong relationship between need state, cue-evoked dopamine activity, and subsequent approach and consumption suggests that the dopamine response invigorates appropriate behaviors to restore homeostatic balance.

Central AngII Is Sufficient to Recruit Cue-Evoked Phasic VTA Dopamine Neuron Activity. Physiological need, including thirst, triggers signaling cascades originating in the periphery that act centrally for need-state detection and the command of appropriate goal-directed action. The renin–angiotensin cascade is a canonical response to a decrease in blood volume (5). Other hormones, such as stomach-derived ghrelin, are released in response to energy imbalance (45–47). Central delivery of these hormones increases fluid (AngII) and food (ghrelin) consumption, respectively (48, 49). We conditioned thirsty rats to associate a cue with water availability. After 2 d of ad libitum access to water, rats ($n = 14$) received a central infusion of either AngII (10 ng/μL, intracerebroventricular [ICV], administered immediately prior to test session) (49) or

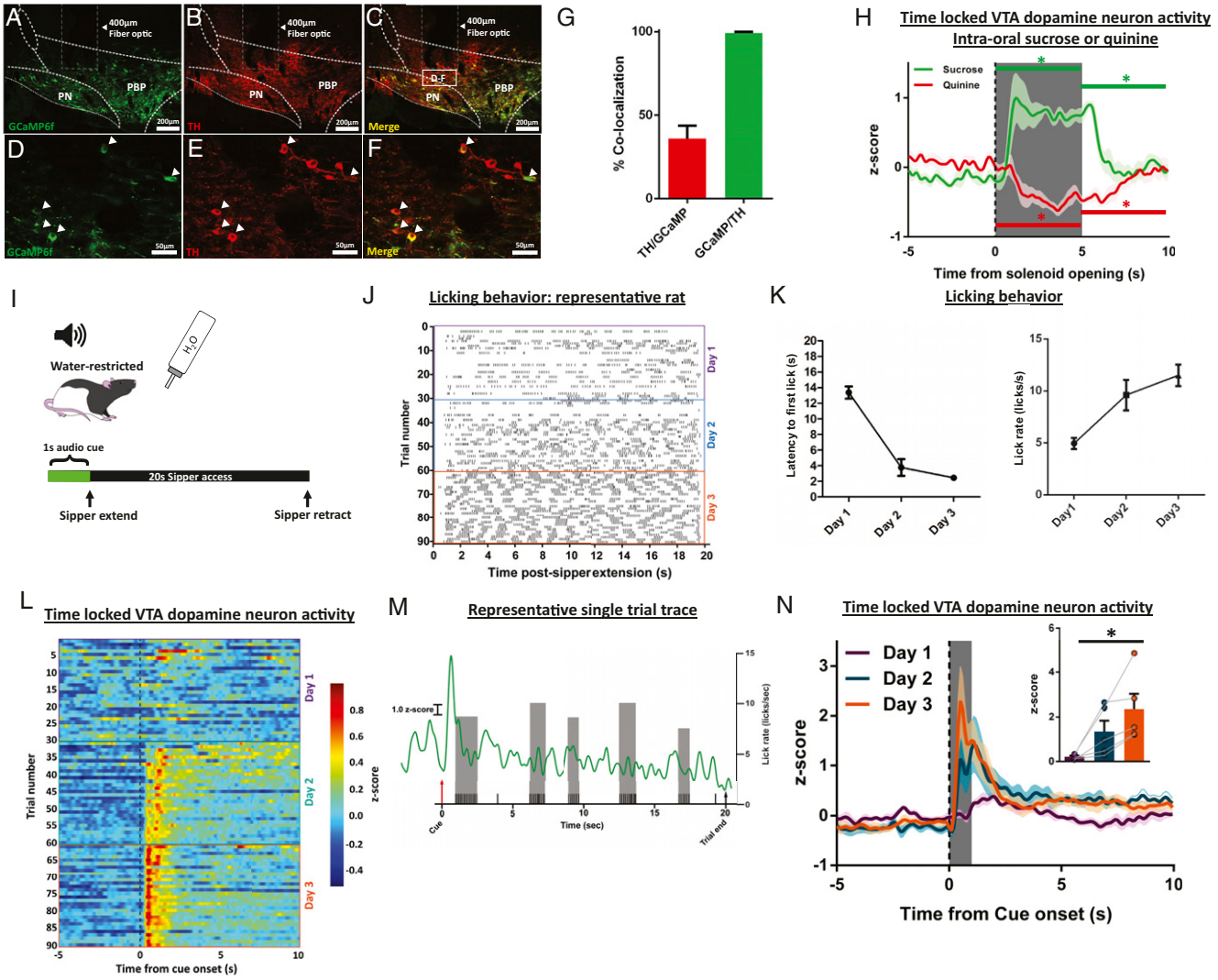

Fig. 1. In vivo fiber photometry in the mesolimbic dopamine system captures phasic dopamine responses to cues that predict water. (*A–F*) Representative images showing Cre-dependent GCaMP6f expression (*A*, green) in VTA dopamine neurons labeled with TH (*B*, red; *C*, yellow merge; white box labeled *D–F* indicates area of higher magnification in *D–F*). Higher magnification *Insets* are shown in *D–F*, white arrows indicate gCaMP-positive neurons colocalized with TH. (*G*) Quantification of TH-expressing neurons that are also labeled for GCaMP (penetrance, red bar) and GcaMP-expressing neurons that are also labeled for TH (selectivity, green bar). (*H*) VTA dopamine neuron activity time locked to intraoral infusion of sucrose or quinine (−5 to 10 s relative to the start [dotted vertical line] of the 5-s intraoral infusion [gray box]). Horizontal bars (green, sucrose; red, quinine) above the trace represent 5-s bins where dopamine activity is significantly different vs. baseline, $*P < 0.05$. (*I*) Schematic of the water-cue sipper behavioral paradigm. (*J*) Licking behavior during training in a representative rat. (*K*) Training. Average latencies to first lick (*Left*) and lick rate in first licking bout (*Right*). (*L*) Average ($n = 5$ rats) VTA dopamine neuron activity (in color) across trials during the seconds before and after cue onset ($t = 0$ s). (*M*) Single trial dopamine activity trace from a representative rat with licks (black ticks). Gray bars are lick rates within each lick bout (1 bout, series of licks that precede a pause greater than 500 ms). (*N*) Average VTA dopamine neuron activity time locked to cue onset (dotted line) with quantification in the *Inset*. Dark lines in *H* and *N* are means and shading are ±SEM. Bars and whiskers are means±SEM. Gray bar in *N* represents quantification time window (1-s postcue onset) shown in the *Inset*. $*P < 0.05$; main effect of day.

vehicle (veh) in a counterbalanced, within-subject design. We compared the dopamine response to the water-predictive cue on the final day of training (when rats were water deprived) with both treatment conditions when rats were in a euvolemic state. Relative to the vehicle condition, both water deprivation and central AngII under ad libitum conditions significantly augmented the phasic dopamine response aligned to the onset of the water-predictive cue or first lick [cue: Fig. 3*A*; quantification in Fig. 3*B*, $F(2, 26) = 10.81$, $P = 0.0004$ (treatment); veh vs. AngII $P = 0.0004$, veh vs. water dep $P = 0.0054$, AngII vs. water dep $P = 0.5925$; first lick: *SI Appendix*, Fig. S2*E*; $F(2, 26) = 6.856$, $P = 0.0041$; veh vs. AngII $P = 0.0031$, veh vs. water dep $P = 0.0714$, AngII vs. water dep $P = 0.3834$]. Thus, central AngII in the euvolemic state recapitulated the effects of water deprivation. Effects on dopamine signaling were mirrored in behavioral responses. Relative to euvolemia, latency to first lick was reduced and lick rate was increased by AngII treatment [latency: Fig. 3 *C*, *Left*: $F(2, 26) = 22.92$, $P < 0.0001$, veh vs. AngII $P < 0.0001$, veh vs. water dep $P < 0.0001$, AngII vs. water dep $P = 0.7336$; lick rate in the first bout: Fig. 3 *C*, *Right*: $F(2, 26) = 7.796$, $P = 0.0022$; veh vs. AngII $P = 0.0087$, veh vs. water dep $P = 0.0039$, AngII vs. water dep $P = 0.9435$; *SI Appendix*, Table S1].

To determine if the effect of hormone delivery was specific for a thirst signal, we conditioned another group of thirsty rats ($n = 4$) to associate a cue with water availability. After 2 d of ad libitum access, we centrally administered the "hunger" hormone ghrelin (1 μg/μL, ICV) (48) or vehicle immediately prior to the recording session in a within-subjects, counterbalanced design.

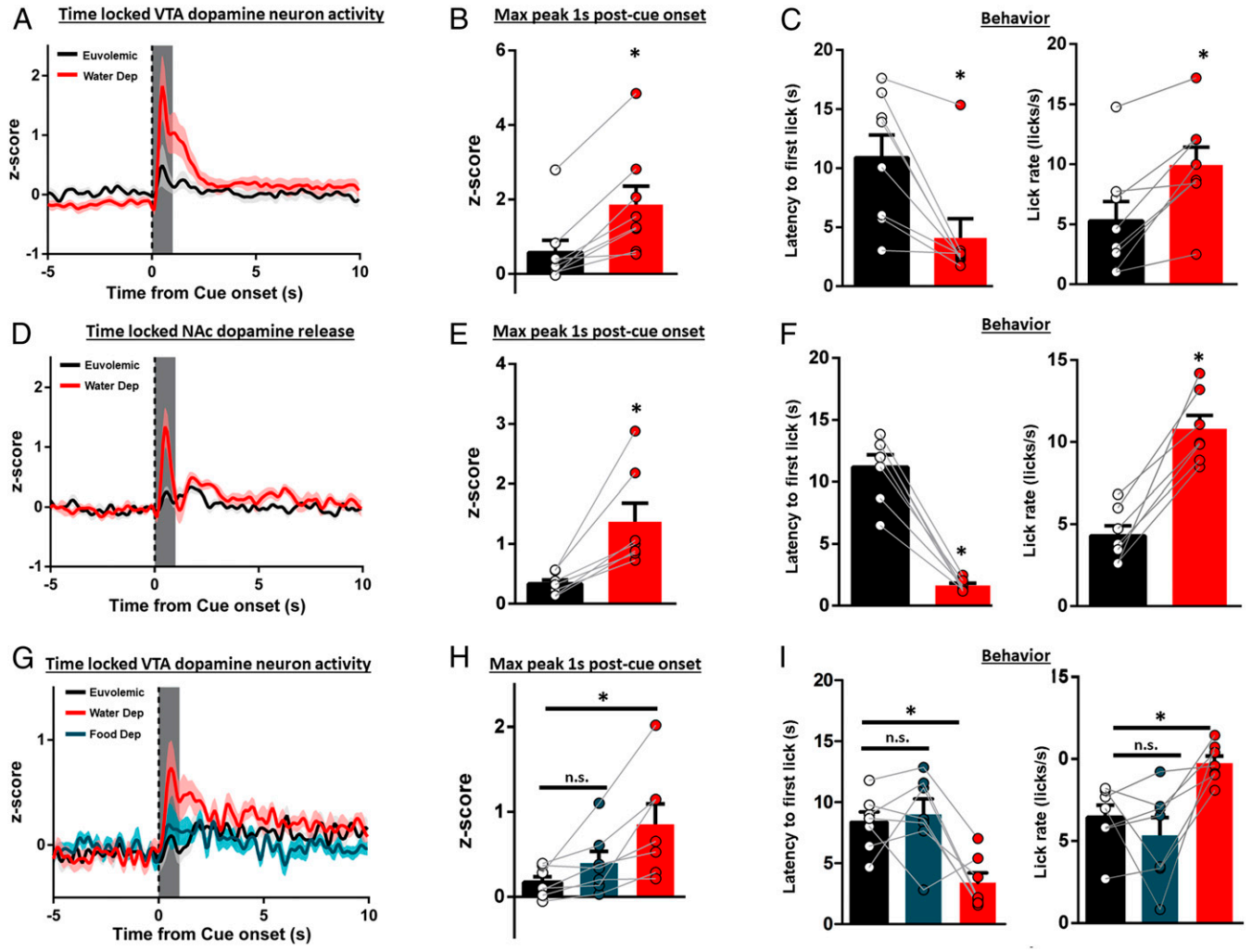

Fig. 2. Water-cue-evoked phasic dopamine activity is dependent on physiological state. (*A*) VTA dopamine neuron activity time locked to water-cue presentation (dotted line) in euvolemic (ad libitum fed/watered) or water-deprived rats with quantification in *B*. (*C*) Latency to first lick and lick rate in euvolemic or water-deprived rats from *A* and *B*. (*D*) NAc dopamine release time locked to water-cue presentation in euvolemic or water-deprived rats with quantification in *E*. (*F*) Latency to first lick and lick rate in euvolemic or water-deprived rats from *D*–*E*. (*G*) VTA dopamine neuron activity time locked to water-cue presentation in euvolemic, overnight food-deprived, or overnight water-deprived rats with quantification in *H*. (*I*) Latency to first lick and lick rate in euvolemic, food-deprived, or water-deprived rats from *G* and *H*. Dark lines in *A*, *D*, and *G* are means and shading are ±SEM. Bars and whiskers in *B*, *E*, and *H* are means ±SEM. Gray boxes in *B*, *E*, and *H* represent 1-s time window postcue onset for quantification and analysis. $*P < 0.05$ vs. euvolemic. n.s., not significant vs. euvolemic.

Unlike AngII, ghrelin failed to potentiate either cue or first lick-evoked phasic dopamine responses relative to vehicle. Importantly, in these same rats, water deprivation did potentiate the dopamine response, relative to either treatment [Fig. 3*D*; quantification in Fig. 3*E*: $F(2, 6) = 68.24$, $P < 0.0001$, veh vs. ghrelin $P = 0.8185$; veh vs. water dep, $P = 0.0002$; ghrelin vs. water dep $P = 0.0001$; *SI Appendix*, Fig. S2*F*: $F(2, 6) = 11.72$, $P = 0.0085$, veh vs. ghrelin $P = 0.8308$; veh vs. water dep, $P = 0.0194$; ghrelin vs. water dep $P = 0.0102$] further supporting selective recruitment of the mesolimbic dopamine system to engage the appropriate goal-directed behavior. Latency to first lick and lick rate were not affected by ghrelin [latency: Fig. 3 *F*, *Left*: $F(2, 6) = 11.72$, $P = 0.0085$, veh vs. ghrelin $P = 0.8308$; veh vs. water dep, $P = 0.0194$; ghrelin vs. water dep $P = 0.0102$; lick rate in first bout: Fig. 3 *F*, *Right*: $F(2, 6) = 21.17$, $P = 0.0102$, veh vs. ghrelin $P = 0.9909$; veh vs. water dep, $P = 0.0380$; ghrelin vs. water dep $P = 0.0313$].

SFO^{CaMKIIa} Activity Is Necessary and Sufficient for Water-Cue-Evoked VTA Dopamine Neuron Activity. The SFO has a fenestrated blood–brain barrier (50) and exhibits a robust response to dehydration and AngII (4, 6–9, 51). Activation of SFO neurons through expression of Gq-coupled DREADDs under control of the CaMKIIa promoter potently stimulates fluid consumption in euvolemic mice (10). As thirst (or AngII in euvolemia) recruits phasic dopamine signaling in response to a water-predictive cue, we hypothesized that SFO^{CaMKIIa} neurons were critical mediators of this interaction. To address this, we combined selective, chemogenetic activation/inhibition of SFO^{CaMKIIa} neurons using DREADDs [Fig. 4 *A*–*M*; cFos validation in Fig. 4 *N*–*P*, $t(7) = 4.108$, $P = 0.0045$ veh vs. clozapine-n oxide (CNO)] in conjunction with in vivo fiber photometry recording from VTA dopamine neurons. Consistent with previous work (10), activation (Gq-DREADD expression) of SFO^{CaMKIIa} with CNO (1 μg/μL, ICV) in euvolemic rats ($n = 10$) significantly increased water intake relative to vehicle [Fig. 4*Q*; $t(9) = 4.692$, $P = 0.0011$], while in a separate cohort of water-deprived rats ($n = 8$), inhibition (Gi-DREADD expression) of SFO^{CaMKIIa} decreased water intake [Fig. 4*R*; $t(7) = 3.054$, $P = 0.0185$]. Next, we trained the same rats (SFO^{CaMKIIa} hM3Dq or hM4Di transfected) while water restricted to associate a cue with

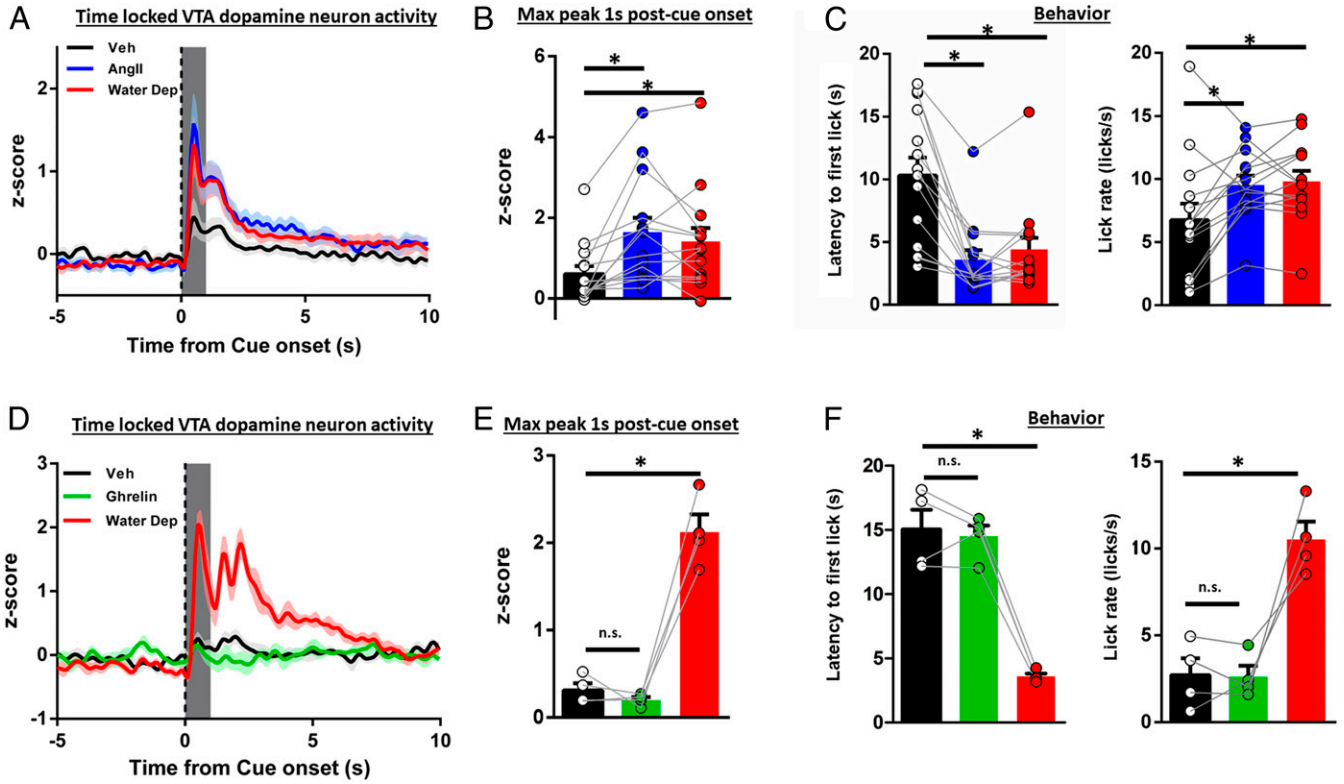

Fig. 3. Central administration of AngII, but not ghrelin, potentiates water-cue-evoked phasic dopamine signaling in euvolemic rats. (*A*) VTA dopamine neuron activity time locked to cue onset ($t = 0$) in euvolemic vehicle, euvolemic AngII (10 ng/μL), or overnight water-deprived rats with quantification in *B*. (*C*) Latency to first lick and lick rate in euvolemic vehicle, euvolemic AngII, or water-deprived rats from *A* and *B*. (*D*) VTA dopamine neuron activity time locked to cue onset ($t = 0$) in euvolemic vehicle, euvolemic ghrelin (1 μg/μL) or overnight water-deprived rats with quantification in *E*. (*F*) Latency to first lick and lick rate in euvolemic vehicle, euvolemic ghrelin, or water-deprived rats from *D*–*E*. Dark lines in *A* and *D* are means and shading are ±SEM. Bars and whiskers in *Insets* are means ±SEM. Gray boxes in *B* and *E* represent 1-s time window postcue onset for quantification and analysis. *$P < 0.05$ vs. veh. n.s., not significant vs. veh.

water availability and measured VTA phasic dopamine activity when rats were thirsty or euvolemic (within-subjects design, counterbalanced across treatment). In euvolemic rats, CNO treatment to activate SFO^{CaMKIIa} neurons significantly potentiated cue and first-lick-evoked VTA dopamine neuron activity, relative to vehicle treatment [cue: Fig. 4*S*; quantification in Fig. 4*T*: $t(9) = 4.215$, $P = 0.0023$ CNO vs. veh; first lick: *SI Appendix*, Fig. S2*G*; $t(9) = 3.057$, $P = 0.0136$; CNO administered 20 min prior to session]. Moreover, SFO^{CaMKIIa} activation was sufficient to increase behavioral responses for water [latency: Fig. 4 *U*, *Left*: $t(9) = 3.982$, $P = 0.0032$; lick rate in first bout: Fig. 4 *U*, *Right*: $t(9) = 3.110$, $P = 0.0125$]. Illustrating bidirectional control, CNO treatment to suppress SFO^{CaMKIIa} activity in water-deprived rats significantly attenuated cue-evoked VTA dopamine neuron activity relative to vehicle treatment [Fig. 4*V*; quantification in Fig. 4*W*: $t(7) = 3.966$, $P = 0.0054$ veh vs. CNO]; however, treatment was without effect when dopamine neuron activity was aligned to first lick [*SI Appendix*, Fig. S2*H*; $t(7) = 0.8103$, $P = 0.4445$] and had no impact on behavioral responses for water [latency: Fig. 4 *X*, *Left*: $t(7) = 1.701$, $P = 0.1327$; lick rate in first bout: Fig. 4 *X*, *Right*: $t(7) = 0.9320$, $P = 0.3824$]. These effects are not due to CNO administration alone, as CNO delivery in rats expressing a fluorophore in the SFO ($n = 3$) was without effect on behavior or cue-evoked VTA dopamine neuron activity in either the euvolemic or water-deprived state [*SI Appendix*, Fig. S4*A*, $F(1, 2) = 38.14$, $P = 0.0252$ (state); $F(1, 2) = 0.7288$, $P = 0.4832$ (drug); $F(1, 2) = 0.1010$, $P = 0.7807$ (state by drug); *SI Appendix*, Fig. S4*B* and Table S1]. Collectively, results identify central first-order homeostatic neurons as integrators of peripheral signals that can strongly influence mesolimbic dopamine signaling and subsequent approach behaviors.

Phasic Dopamine Responses to Cues Are Sustained across the Recording Session. Previous work has shown that excitatory SFO neurons are active in the thirsty mice but exhibit a rapid (on the order of seconds) decrease in activity that can begin in anticipation of access to water. This rapid decay occurs before changes in plasma osmolality (11). Given the rapid decrease in excitatory SFO activity upon access to water and the relationship between SFO^{CaMKIIa} neurons and phasic dopamine activity observed here, we investigated whether the phasic dopamine response to water-predictive cues varies over the course of a behavioral session. Analyzing dopamine responses to the water-predictive cue on a trial-by-trial basis in thirsty rats ($n = 8$), we observed no appreciable change in signal as rats progress through trials (Fig. 5*A*, color plot showing mean cue-evoked signal across trials). This was supported by a poor correlation between trial number and the magnitude of the water-cue-evoked signal (Fig. 5*B*; slope = –0.0014, $r^2 = 0.0033$, $P = 0.7611$). Thirsty rats exhibit largely short latencies to first lick (distribution in Fig. 5*C*) that is sustained throughout the session. Indeed, there was no correlation between trial number and latency (Fig. 5*D*; slope = –0.0237 $r^2 = 0.0243$, $P = 0.4102$), indicating that water and the cue that predicted it continued to have a strong motivating influence on behavior throughout the session. Thus, unlike the properties of excitatory SFO neurons, VTA dopamine neurons in the thirsty state exhibit canonical phasic activity in response to cues that predict water—activity

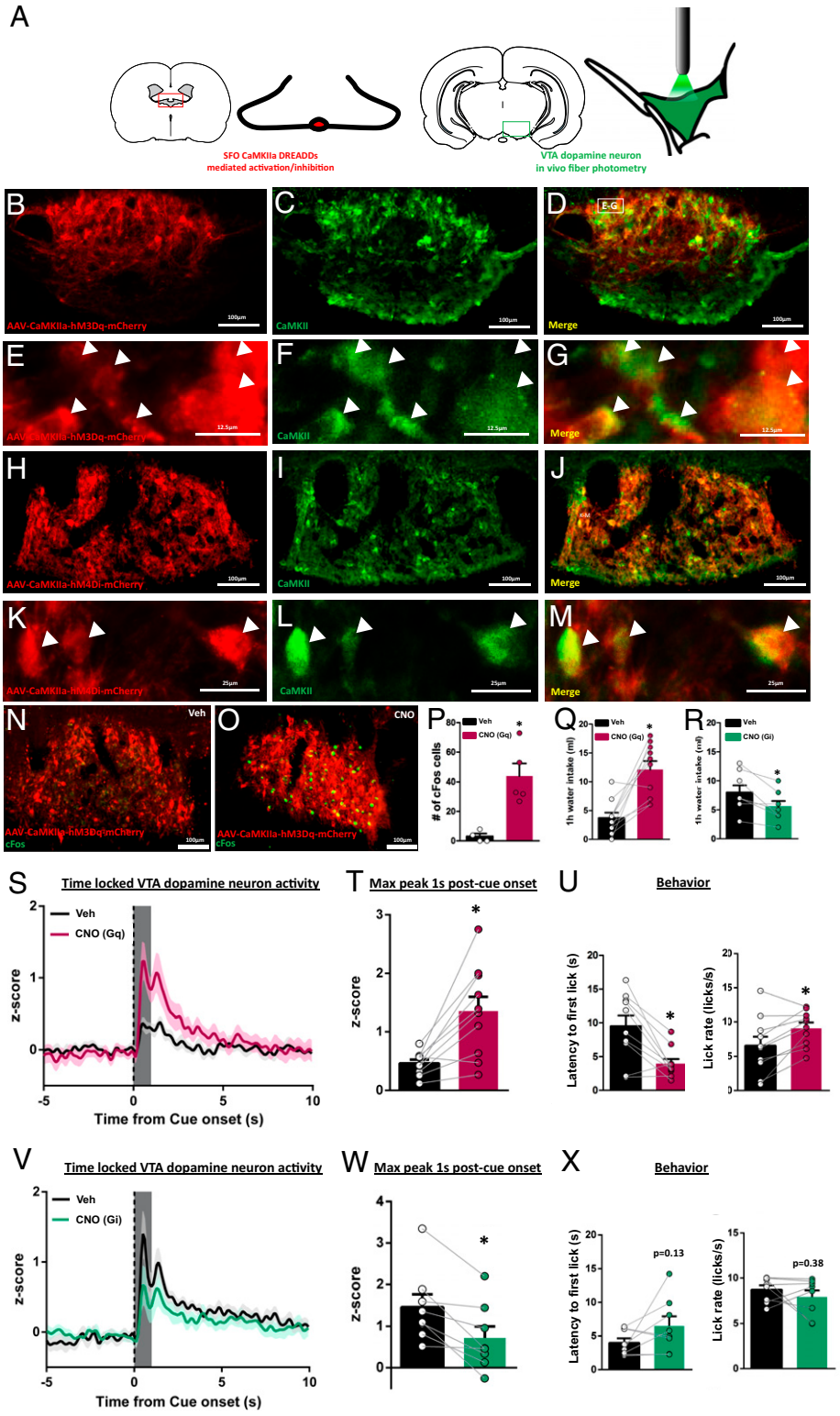

Fig. 4. SFO^{CaMKIIa} activity is necessary and sufficient for water-cue-evoked VTA dopamine neuron activity. (*A*) Experimental design using a combination of selective manipulation of SFO^{CaMKIIa} with DREADDs and in vivo fiber photometry from VTA dopamine neurons. (*B–M*) Representative images of SFO CaMKIIa-hM3Dq-mCherry (*B–G*) or CaMKIIa-hM4di (*H–M*) (red) and CaMKII expression (green). High-magnification *Insets* are shown in *E–G* and *K–M* with white arrows showing DREADD and CaMKII colocalization. (*N* and *O*) cFos expression (green) following vehicle or CNO (1 μg/μL) in CaMKIIa-hM3Dq transfected SFO neurons and quantification in *P*. (*Q* and *R*) One-hour water intake following vehicle or CNO treatment in (*Q*) SFO CaMKIIa-hM3Dq (euvolemic) or (*R*) SFO CaMKIIa-hM4Di (water-restricted) transfected rats. (*S*) VTA dopamine neuron activity in euvolemic, CaMKIIa-hM3Dq transfected rats following vehicle or CNO treatment ($t = 0$ for cue onset) with quantification in *T*. (*U*) Latency to first lick and lick rate in euvolemic vehicle or euvolemic CNO rats from *S* and *T*. (*V*) VTA dopamine neuron activity in water-restricted, CaMKIIa-hM4Di transfected rats following vehicle or CNO treatment ($t = 0$ for cue onset) with quantification in *W*. (*X*) Latency to first lick and lick rate in water-restricted vehicle or water-restricted CNO rats from *V–W*. Dark lines in *S* and *V* are means and shading are ±SEM. Bars and whiskers in all graphs are means ±SEM. Gray boxes in *T* and *W* represent 1-s time window postcue onset for quantification and analysis. *$P < 0.05$ vs. vehicle.

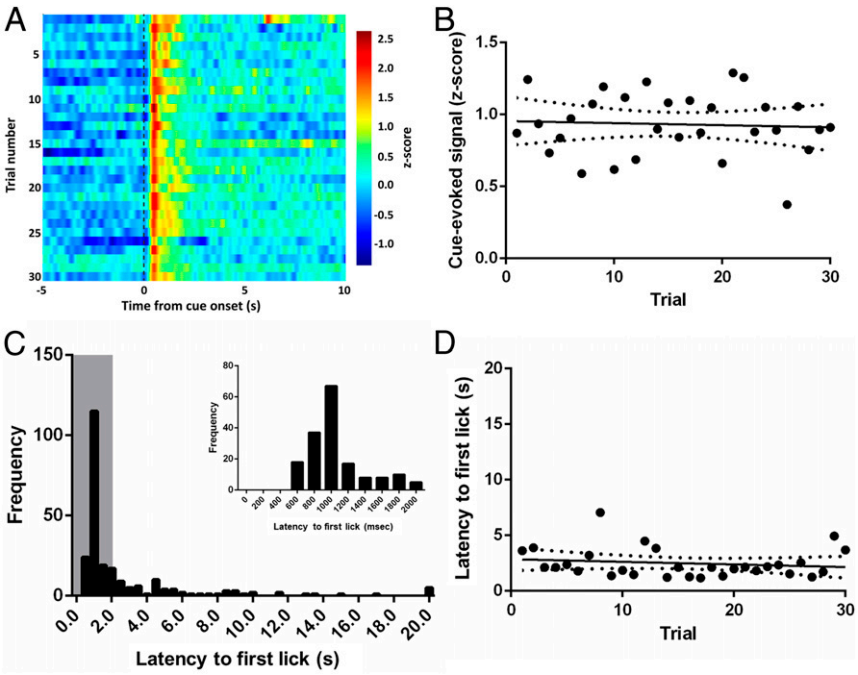

Fig. 5. Phasic dopamine responses to cues and behavior in thirsty rats are sustained across the recording session. (*A*) VTA dopamine neuron activity (color) during 15-s window around cue (−5 to +10 s relative to cue onset) across trials. (*B*) Correlation between cue-evoked signal and number of trials, slope = −0.0014, r^2 = 0.0033, P = 0.7611. (*C*) Distribution of first lick latencies from all rats. Gray box indicates time window for *Inset* showing the same distribution through 2 s with 200-ms bins. (*D*) Correlation between latency and trial number (maximum latency per trial = 20 s), slope = −0.0237 r^2 = 0.0243, P = 0.4102.

that does not quench as rats progress through a behavioral session that lasts on the order of minutes.

Changes in Phasic Dopamine Account for Behavioral Changes across Treatments. The current results suggest that cue-evoked dopamine responses, which peak prior to spout availability, are related to behavioral responses to the cue (e.g., approach as indexed by latency) and spout availability (e.g., lick rate). Since all experiments were conducted within-subjects, we quantified how much the phasic dopamine responses, latency to first lick, and lick rate in first bout changed from the control condition in each subject. In this way, the change in dopamine signal—whether due to water deprivation, food deprivation, AngII, ghrelin, or activation/inhibition of SFO^{CaMKIIa} neurons—was standardized across conditions and provided an index for comparisons across treatments. For each z-score increase in dopamine signal, the

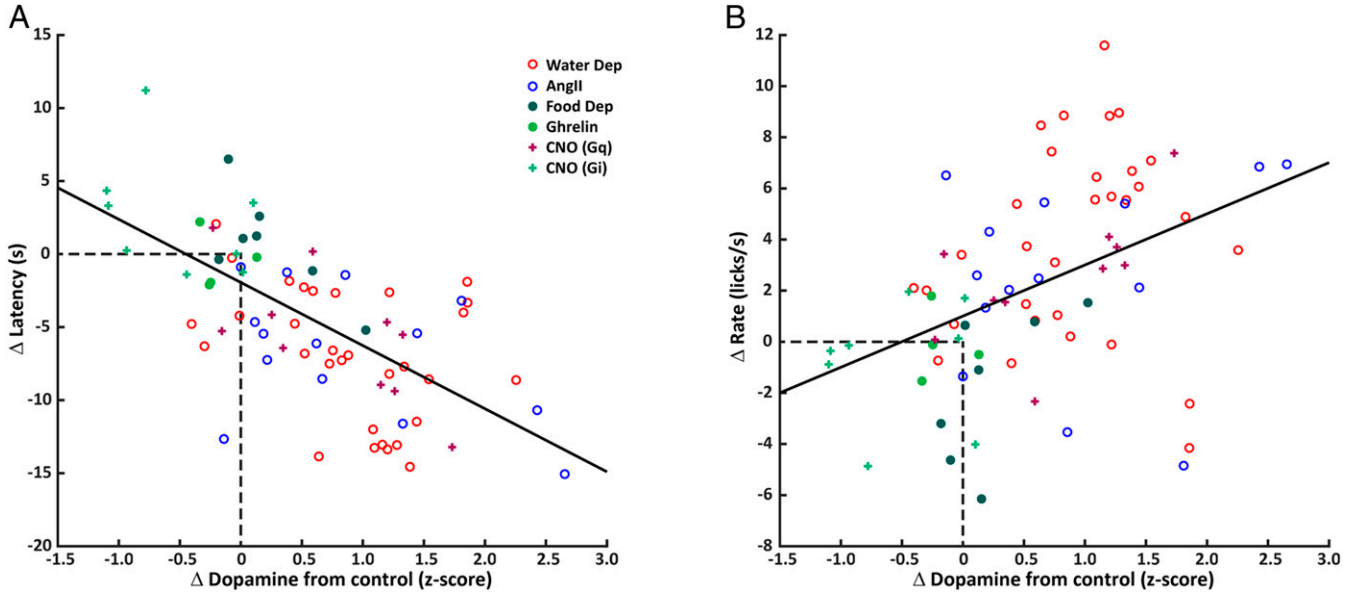

Fig. 6. Changes in phasic dopamine account for behavioral changes across treatments. (*A*) Within-subjects (treatment − control) regression model for Δ latency to first lick and Δ cue-evoked dopamine signal across all treatments, slope = −4.3206, r^2 = 0.4243, P < 0.0001. (*B*) Within-subjects regression model for Δ lick rate in the first bout and Δ cue-evoked dopamine signal across all treatments, slope = 2.0011, r^2 = 0.1849, P = 0.0001.

average latency to first lick decreased 4.3206 s (Fig. 6*A*, treatment indicated by symbols: CI: −5.4864 to −3.1548; $r^2 = 0.4243$, $P < 0.0001$). Increases in dopamine signal were also associated with faster lick rate in the first bout of responding. For each z-score increase in dopamine signal, average lick rate was 2.0011 licks/s faster (Fig. 6*B*: CI: 1.0279 to 2.9744; $r^2 = 0.1849$, $P = 0.0001$). Similar outcomes were observed when measurements of dopamine release (using dLight1.2) were included in the analyses (*SI Appendix*, Fig. S5 and Table S1). The linear relationships between change in dopamine signal and change in behavior suggest that the altered state of the rat alone does not determine behavior, but that individual differences in treatment-induced dopamine signaling are related to the magnitude of the changes in behavior. Overall, water deprivation, AngII, and activation of $SFO^{CaMKIIa}$ neurons resulted in the largest increases in dopamine signal relative to control sessions, corresponding to larger reductions in latency and increases in lick rate. Food deprivation and ghrelin treatment did not result in large changes in dopamine signals nor behavior. Finally, inhibition of $SFO^{CaMKIIa}$ neurons fell along the same continuum with reductions in dopamine compared to vehicle treatment corresponding to longer latencies and slower lick rates.

Discussion

Phasic dopamine activity is associated with unexpected reward and reward-predictive cues (52) but also additional variables that include incentive motivation (18–22) and the invigoration of movement toward rewards (25, 53, 54). Deprivation states (i.e., thirst and hunger) enhance both motivation for (55) and phasic dopamine responses to (28, 31) restorative stimuli or cues that predict them. Here, we show that canonical first order signals (i.e., AngII) and central circuits for thirst (i.e., $SFO^{CaMKIIa}$ neurons) are sufficient and necessary for the tuning of phasic dopamine responses that, in turn, are correlated with enhanced motivation.

Water deprivation potentiated the phasic dopamine response to a water-predictive cue. This appears to be a highly conserved response as dopamine neurons of *Drosophila* exhibit similar state-dependent responses to water-related stimuli (56, 57). The augmented dopamine response to the water-associated cue was dependent on the type of physiological need as hunger had no impact. Collectively, our results support parallel channels of information that relate physiological state to midbrain dopamine neurons. Each channel can be selectively activated by internal milieu and homeostatic circuits that detect changes in the internal milieu.

In general, we find that the degree of behavioral output (i.e., latency to first lick and lick rate) is dependent on the magnitude of cue-evoked dopamine signals, where larger cue-evoked dopamine activity is predictive of decreased latency to first lick and increased lick rate. Critically, taking advantage of our within-subjects design to convert data across experiments into a common metric, we show that this relationship is consistent across changes in need states via water deprivation, thirst induction through AngII pharmacology, and $SFO^{CaMKIIa}$ chemogenetics, with larger changes in dopamine responses relating to greater reductions in latency and greater increases in lick rate. Specific deprivation states, or activation of neurons that relate specific deprivation states, can alter competition between motivated behaviors to bias toward those that restore homeostasis (55). We also observed elevated first-lick-evoked dopamine responses in thirsty rats, suggesting that deprivation states modulate consummatory behaviors—data consistent with prior work (31, 32, 58). A notable exception to the relationships described above, while water deprivation modulated the magnitude of water-cue-evoked dopamine release in the NAc dorsomedial shell, it had no effect on dopamine levels related to first lick. Phasic dopamine release in different subterritories of the NAc play varying roles in behavior (14, 35). Our VTA fiber optic placement (primarily in the parabrachial pontine tegmental nucleus—which projects primarily to the lateral NAc shell) may very well have captured dopamine cell body populations that contribute to different aspects of behavior than those that terminate in the NAc dorsomedial shell. Future studies will be required to determine how need states impact NAc dopamine release along the rostral/caudal and medial/lateral axes of the VTA and dopamine terminal regions.

Supporting the idea that internal milieu selectively recruits dopamine activity, over 25 y ago Hoebel et al. used euvolemic rats and demonstrated that central administration of AngII increased extracellular dopamine in the NAc. The dopamine response was even greater if rats had access to water (59). Our results extend these findings to include AngII potentiation of transient spikes in dopamine activity evoked by water-predictive cues. Presumably, the enhanced dopamine response under the influence of AngII promotes approach and consumption. Indeed, the predictive relationships between the change in magnitude of cue-evoked dopamine and the change in behavior (e.g., latency to first lick and lick rate) with AngII administration overlapped well with that observed following water deprivation (Fig. 6, red versus blue open circles). Central delivery of ghrelin, normally released by the stomach and acting centrally to promote feeding, had no effect on phasic dopamine responses to the water-predictive cue—once again arguing for parallel channels by which physiological state recruits dopamine responses to cues in the service of motivation.

One mechanism for the recruitment of phasic dopamine responses to learned environmental stimuli in times of need is direct hormone action on dopamine neurons. Indeed, VTA dopamine neurons express receptors for and respond to hormones of peripheral origin (60–67). In response to dehydration, AngII acts via central angiotensin AT1 receptors—expressed throughout the brain—to promote fluid consumption (68). However, there is little to no expression of AT1 within the VTA or NAc (68) and there is no evidence for direct action of AngII in the VTA in the context of thirst-motivated behaviors. In contrast, AngII acts directly on circumventricular organs, the lamina terminalis, and the SFO in particular (4, 7–9, 51) to rapidly promote the consumption of water. Glutamatergic SFO neurons overlap significantly with those that express CaMKIIa or neural nitric oxide synthase (nNOS). These SFO populations are active following dehydration or AngII administration (11). Activation of $SFO^{CaMKIIa}$ or SFO^{nNOS} neurons produces dramatic water consumption in euvolemic mice (9, 10). We found that activation of $SFO^{CaMKIIa}$ in euvolemic rats was sufficient to promote avid water consumption, cue-induced approach behavior, and water-cue-evoked phasic dopamine activity. In water-deprived rats, inhibition of $SFO^{CaMKIIa}$ blunted water consumption and the phasic dopamine response to a water-predictive cue. Intriguingly, $SFO^{CamKIIa}$ inhibition did not reduce dopamine signaling to the level of euvolemic rats and had no effects on first-lick-evoked responses. It is important to recognize that other regions of the lamina terminalis respond to dehydration signals in concert with the SFO (6) and could account for the residual dopamine response.

Historically, central nodes for motivation have been segregated into homeostatic versus hedonic mediators. This dichotomy is becoming increasingly blurred (69–71). Here, we demonstrate clear communication between central first order detectors of body fluid imbalance in the SFO and phasic dopamine responses that promote and reinforce behavior. There are no known direct projections from the SFO to the VTA. Considerable work has identified projections within the lamina terminalis that mediate thirst and the quenching of thirst (6, 72). Output from the lamina terminalis can reach targets that, in turn, project to the VTA. One promising intermediary between the lamina terminalis and VTA dopamine neurons is the lateral hypothalamic area (LHA). The SFO projects directly and indirectly (via the MnPO) (73) to the

LHA (74, 75). Moreover, while output targets from the lamina terminalis uniformly promote drinking, they differentially affect autonomic and motivational output—with the LHA as a key target for the latter (73). The LHA contains populations of neurons that promote fluid consumption. For example, activation of LHA neurotensin neurons promotes robust fluid consumption (76), although these neurons do not appear to project directly to the VTA (77). Alternatively, the lamina terminalis projects to LHA orexin neurons that, in turn, do project to the VTA and mediate water-drinking behaviors (78). Orexin has long been known to modulate dopamine neural activity in the context of hunger (79). Thus, separate populations of LHA orexin neurons that project to the VTA have the potential to serve as parallel channels to invigorate appropriate goal-directed actions. Functionally mapping this circuit will further elucidate the cellular and integrative mechanisms by which deviations in homeostasis recruit motivated behavior.

Activity of excitatory SFO neurons is elevated in thirsty animals but activity is quenched rapidly in anticipation of rehydration but before changes in plasma osmolality take place (9), suggesting that SFO neurons "anticipate" later homeostatic restoration (11). We found that the potentiation of cue-evoked phasic dopamine activity and approach behavior in thirsty animals is sustained throughout the behavioral session. The apparent mismatch in time course for first order homeostatic neural activity and motivation is consistent with work performed in the context of hunger. Like SFO neurons, activity of AgRP neurons in the arcuate nucleus is high but is rapidly quenched by food cues and before calorie absorption (80). Interestingly, brief optogenetic stimulation of AgRP neurons prior to food availability imparts long-lasting enhancement of appetitive and consummatory behaviors (81). Initial learning of cue-outcome associations under deprivation states could lead to residual responses under homeostasis that bias behavior toward approach. Indeed, here, the water-predictive cue still evoked a phasic dopamine response in euvolemia. This residual dopamine response could contribute to continued approach in the absence of need, leading to overconsumption and maladaptive states.

The current data highlight the critical notion that the neural substrates that regulate homeostatic balance and those that mediate goal-directed behaviors are intimately linked. The results provided here identify peripheral regulators of need (AngII) that communicate to central need state detectors (SFO) that in turn engage the mesolimbic dopamine system to facilitate motivation. We provide foundations through which other types of physiological need (e.g., hunger) might communicate to the mesolimbic dopamine system and demonstrate the powerful capabilities of phasic dopamine signaling to engage appropriate—and highly selective—goal-directed behaviors.

Materials and Methods

Animals. We used male and female (randomly cycling) Long Evans rats (>250 g) expressing Cre recombinase under the control of the tyrosine hydroxylase promoter [TH:Cre$^+$ (26); Rat Research Resource Center, RRRC No. 659] or wild-type Long Evans rats. Subjects were individually housed after weaning within a temperature- and humidity-controlled room and on a 12:12 h light:dark schedule (lights on 0700 h). All experiments were conducted in the light cycle. Rats were maintained on ad libitum food and water unless otherwise noted. Data were obtained from a total of 87 animals ($n = 38$ males, $n = 43$ females). A total number of 11 animals were removed because of misplaced fiber optic implant or failed construct delivery (see *SI Appendix*, Fig. S1 for fiber optic placement for all experiments). For all surgical procedures, animals were anesthetized with ketamine hydrochloride (100 mg/kg, intraperitoneally [i.p.]) and xylazine hydrochloride (10 mg/kg, i.p.) for stereotaxic surgery, followed by subcutaneous (s.c.) analgesia (0.1 mL of 5 mg/mL meloxicam). Animal care and use was in accordance with the National Institutes for Health Guide for the Care and Use of Laboratory Animals (82) and approved by the Institutional Animal Care and Use Committee at the University of Illinois at Chicago.

Viruses. Experiments involving in vivo fiber photometry utilized AAVs (adeno-associated viruses) packaged with fluorescent protein sensors for either calcium (AAV1.hSyn.Flex.GCaMP6f.WPRE.SV40; 5×10^{12} GC/mL, Addgene) or dopamine (AAV5.hSyn.dLight1.2; 1.7×10^{10} GC/mL, Addgene). For experiments employing chemogenetic activation or inhibition, the following DREADDs were used: AAV5.CaMKIIa.hM3Dq.mCherry (2×10^{12} GC/mL), AAV5.CaMKIIa.hM4Di (7×10^{12} GC/mL), and AAV5.CaMKIIa.EGFP (blank control virus; 3×10^{12} GC/mL).

Surgeries. For the recording of dopamine neuron activity in the VTA, AAV1.hSyn.Flex.GCaMP6f.WPRE.SV40 was targeted to the VTA of TH:Cre$^+$ animals (1 μL; AP (anterior-posterior) −5.4, ML (medial-lateral) −0.7, DV (dorsal-ventral) −8.15, mm relative to bregma) at a rate of 0.1 μL/min and a 5-min postinfusion period to allow for diffusion. Then, an optic fiber (flat 400-μm core, 0.48 numerical aperture [NA], Doric Lenses Inc.) was implanted in the VTA above the injection site (AP −5.4, ML −0.7, DV −8.00 mm). Experiments involving intraoral infusions of sucrose or quinine included, in addition to fiber photometry preparation, implantation of an intraoral catheter composed of an ∼6-cm length of PE6 tubing (Scientific Commodities, Inc.) that is bordered at one end with a Teflon washer. The catheter was inserted just lateral to the first maxillary molar such that the Teflon washer rests flush against it. The other end was exteriorized out of an incision at the top of the head and held in place with dental acrylic. For the recording of NAc dopamine release, AAV.hSyn.dLight1.2 (34) was infused unilaterally to the dorsomedial NAc shell (1 μL; AP +1.5, ML +0.9, DV −6.8 mm), followed by an optic fiber implanted above the injection site (AP +1.5, ML +0.9, DV −6.7 mm). All experiments involving central drug injections included a chronic indwelling guide cannula (26 Ga Cannula, PlasticsOne) implanted above the lateral ventricle (ICV; AP −0.9, ML −1.8, DV: −2.6 mm relative to bregma).

All experiments involving DREADD-mediated chemogenetic manipulations included either AAV5.CaMKIIa.hM3Dq.mCherry, AA5.CaMKIIa.hM4di.mCherry, or AAV5.CaMKIIa.EGFP targeted to the SFO (200 nL at 0.1 μL/min; AP −1.0 ML 0, DV −4.9 mm). Animals recovered for 2 wk to allow for construct expression. Animals were removed from the study if mCherry expression spread outside of the SFO ($n = 2$ removed).

Central Drug Injections. Experiments involving infusions into the lateral ventricle included injections of Angiotensin II (10 ng/ μL; Bachem), ghrelin (1 μg/μL; Bachem), or CNO (1 μg/μL, Tocris). Drugs were dissolved in artificial cerebral spinal fluid (aCSF). Drugs were administered with a 33-gauge microsyringe injector (Hamilton) that projected 2 mm beyond the guide cannula. All pharmacological treatments were performed in a counterbalanced, within-subjects design.

In Vivo Fiber Photometry. In vivo fiber photometry was performed according to protocols from ref. 30. Briefly, LEDs (light-emitting diodes; Doric Lenses) administered 465 nm (Ca^{2+} or dLight-dependent) and 405 nm (Ca^{2+} or dLight-independent) excitation. Intensity of the 465 nm and 405 nm light was sinusoidally modulated at 211 Hz and 531 Hz, respectively, for all recording sessions. Light was coupled to a filter cube (FMC4, Doric Lenses) and converged into an optical fiber patch cord mated to the fiber optic implant of the animal. Fluorescence was collected by the same fiber/patch cord and focused onto a photoreceiver (Visible Femtowatt Photoreceiver Model 2151, Newport). A lock-in amplifier and data acquisition system (RZ5P; Tucker Davis Technologies), was used to demodulate the fluorescence due to 465-nm and 405-nm excitation. Behavioral events (e.g., cue, licks) were sent as time-stamped TTL (transistor-transistor logic) to the same data acquisition system and recorded in software (Synapse Suite, Tucker Davis Technologies). A Fourier transformed subtraction was used to account for movement artifacts and bleaching (ΔF/F). The subtracted signal was smoothed using a custom fifth order bandpass Butterworth filter (cutoff frequencies: 0.05 Hz, 2.25 Hz).

To compare task-related responses across recording sessions, the smoothed Fourier-subtracted signal of each session was normalized by each session's average fluorescence and SD to convert data to z-scores. The normalized signal was then aligned to behavioral events of interest (cues, licks). All data have been made available in the supplemental information.

Immunohistochemistry. Following completion of experiments, rats were anesthetized with sodium pentobarbital (100 mg/kg) and transcardially perfused with 0.01 M PBS (phosphate-buffered saline) followed by 10% buffered formalin solution (HT501320, Sigma Aldrich). Brains were removed and stored in formalin with 20% sucrose. All brains were sectioned at 30 μm on a freezing stage microtome (SM2010R, Leica Biosystems). Sections were collected and processed to label for GFP (as an indicator of GCaMP6f or

dLight1.2 expression) and/or TH via immunohistochemistry. Antibodies were incubated at 4 °C (washes and other steps at room temperature). Tissues were permeabilized in 0.3% Triton-X 100 for 30 min and blocked in 2% normal donkey serum for 30 min. Sections were incubated in rabbit anti-TH (AB152, Sigma Aldrich) and/or chicken anti-GFP (AB13907, Abcam) antibodies overnight (~18 h). After KPBS (potassium phosphate-buffered saline) washes (eight changes, 10 min each), secondary antibody (Cy3 conjugated donkey anti-rabbit and AF488 conjugated donkey anti-chicken; Jackson Immunoresearch) was applied and sections were incubated overnight. Sections were then mounted onto glass slides, air dried, and coverslipped with 50% glycerol in KPBS mountant. Only data from subjects with GFP and mCherry expression and correct fiber placement were included in statistical analyses.

Behavior. All training and experimental sessions took place during the light phase in standard operant chambers (ENV-009A-CT, Med Associates Inc.). Water-restricted rats (10 mL water per day) were first habituated to the chamber and the presence of the water sipper (one 30-min session). Then, animals were trained to expect availability of a retractable sipper containing water after the offset of an audio cue (tone; 4.5 kHz, 1-s duration). Licks at the sipper were timestamped using a contact lickometer and controller (ENV-252M; ENV-250, Med Associates Inc.). A trial consisted of the 1-s cue and 20-s sipper availability followed by a randomly selected, variable intertrial interval (32 to 48 s). Daily sessions consisted of 30 trials and continued until behavior stabilized (~3 to 5 d). A separate cohort of animals was trained to expect the availability of a sipper that delivered water after offset of an 1-s audio cue (CS^+; tone or white noise) and another sipper that delivered nothing (CS^-, tone or white noise). Audio cues were counterbalanced between animals, and each daily session consisted of 40 trials (20 CS^+ and 20 CS^-, random order) After training, treatments (drug or deprivation state) were administered in a counterbalanced, within-subjects design with two intervening days between treatments.

For intraoral delivery of sucrose (0.3 M) or quinine (0.0001 M), rats received 30 trials of 5-s fluid infusion (40 μL/s flow rate) with a variable intertrial interval (35 to 55 s). Rats received either sucrose or quinine in a counterbalanced, within-subjects design across 2 d.

Data Analyses. To quantify results from in vivo fiber photometry experiments, the maximum peak 1 s after a behavioral event (e.g., cue presentation, first lick) was measured on each trial and averaged across trials for each session. For intraoral delivery of sucrose/quinine, the mean signal was obtained in 5-s bins before (baseline), during, and after the infusion period (postinfusion). All statistical analyses used one-way or two-way repeated measures analysis of variance (ANOVA) or paired/unpaired *t* tests. When group main effects were found with two or more treatments, Tukey's (for one-way ANOVAs) and Sidak's (for two-way ANOVAs) post hoc tests were employed. Linear regression was used to calculate *P* values, R^2 goodness-of-fit, 95% confidence bands of the best-fit line, and linear equations for trial number vs. average cue-evoked signal. The α-level for significance was 0.05. These statistical analyses were conducted with Prism 5.0 Software (GraphPad Software Inc.).

Regression models were used to test whether differences in licking behavior were related to the changes in the cue-evoked dopamine signal during the treatment condition compared to the control. Two behavioral indices were analyzed separately: latency to the first lick following cue onset for each trial and lick rate in the first burst of licking behavior. Latency was defined as the time interval without a lick following cue onset. In the absence of any licking, this duration was set at 20 s, at which point the spout retracted. The first burst of licking behavior was defined by setting a criterion of 500 ms between two consecutive licks, then dividing the number of licks in the burst by the duration between its first and last lick. If no licks were produced during the trial, lick rate was zero. Analyses completed using a 250-ms interval to define bursts did not yield differences in the results of the regression tests.

We used regression to model the effect of changes in dopamine signals induced by treatment on behavior across conditions. For each animal in each session, we calculated a common metric of dopamine change by taking the difference of average maximum cue-evoked signals (1-s epoch aligned to cue onset) between the treatment (water deprivation, food deprivation, Ang II, ghrelin, or CNO) and corresponding control (euvolemia, vehicle injection) conditions. Similarly, we calculated the change in the latency to first lick and lick rate between the treatment and control sessions for each animal. We estimated the effect of change in cue-evoked dopamine signal on change in behavior across treatments by fitting:

$$Y = b_0 + b_1 D + \varepsilon,$$

where *Y* was change in behavioral index and *D* was the change in maximum z-score signal for cue-evoked dopamine. Regressions were done separately for latency and lick rate. The coefficient b_1 estimated the relationship between the change in dopamine signal and change in behavior, within each subject, from the control to the treatment session. The model also provided an estimate of the correlation between dopamine and behavior (r^2) and the probability (p) that the slope of the best fit did not differ from zero. Regression analyses were conducted with MATLAB R2020a software (Mathworks). Using the average magnitude of the dopamine signal during this 1-s epoch did not alter the main results.

All statistical analyses and values are reported in *SI Appendix*, Table S1.

Data Availability. All study data are included in the article and supporting information.

ACKNOWLEDGMENTS. We thank Dr. James McCutcheon for comments on the manuscript. We also thank the following individuals for assistance with experimental procedures: Rhea Mundle, Brooks Berish, Katya Shcherbyna, Alexandra Crow, and Anthony Ngyuen. This work was funded by NIH grants R01 DA025634 (M.F.R.) and F32 DA047052 (T.M.H.).

1. S. M. Fortin, M. F. Roitman, Physiological state tunes mesolimbic signaling: Lessons from sodium appetite and inspiration from Randall R. Sakai. *Physiol. Behav.* **178**, 21–27 (2017).
2. D. E. Leib, C. A. Zimmerman, Z. A. Knight, Thirst. *Curr. Biol.* **26**, R1260–R1265 (2016).
3. C. Gizowski, C. W. Bourque, The neural basis of homeostatic and anticipatory thirst. *Nat. Rev. Nephrol.* **14**, 11–25 (2018).
4. E. C. Crews, N. E. Rowland, Role of angiotensin in body fluid homeostasis of mice: Effect of losartan on water and NaCl intakes. *Am. J. Physiol. Regul. Integr. Comp. Physiol.* **288**, R638–R644 (2005).
5. J. T. Fitzsimons, Angiotensin, thirst, and sodium appetite. *Physiol. Rev.* **78**, 583–686 (1998).
6. C. A. Zimmerman, D. E. Leib, Z. A. Knight, Neural circuits underlying thirst and fluid homeostasis. *Nat. Rev. Neurosci.* **18**, 459–469 (2017).
7. Z. Xu, J. Xinghong, Drinking and Fos-immunoreactivity in rat brain induced by local injection of angiotensin I into the subfornical organ. *Brain Res.* **817**, 67–74 (1999).
8. B. J. Oldfield, E. Badoer, D. K. Hards, M. J. McKinley, Fos production in retrogradely labelled neurons of the lamina terminalis following intravenous infusion of either hypertonic saline or angiotensin II. *Neuroscience* **60**, 255–262 (1994).
9. Y. Oka, M. Ye, C. S. Zuker, Thirst driving and suppressing signals encoded by distinct neural populations in the brain. *Nature* **520**, 349–352 (2015).
10. H. L. Nation, M. Nicoleau, B. J. Kinsman, K. N. Browning, S. D. Stocker, DREADD-induced activation of subfornical organ neurons stimulates thirst and salt appetite. *J. Neurophysiol.* **115**, 3123–3129 (2016).
11. C. A. Zimmerman *et al.*, Thirst neurons anticipate the homeostatic consequences of eating and drinking. *Nature* **537**, 680–684 (2016).
12. W. E. Allen *et al.*, Thirst regulates motivated behavior through modulation of brainwide neural population dynamics. *Science* **364**, 253 (2019).
13. E. B. Oleson, R. N. Gentry, V. C. Chioma, J. F. Cheer, Subsecond dopamine release in the nucleus accumbens predicts conditioned punishment and its successful avoidance. *J. Neurosci.* **32**, 14804–14808 (2012).
14. M. F. Roitman, R. A. Wheeler, R. M. Wightman, R. M. Carelli, Real-time chemical responses in the nucleus accumbens differentiate rewarding and aversive stimuli. *Nat. Neurosci.* **11**, 1376–1377 (2008).
15. J. E. McCutcheon, S. R. Ebner, A. L. Loriaux, M. F. Roitman, Encoding of aversion by dopamine and the nucleus accumbens. *Front. Neurosci.* **6**, 137 (2012).
16. S. M. Fortin, E. H. Chartoff, M. F. Roitman, The aversive agent lithium chloride suppresses phasic dopamine release through central GLP-1 receptors. *Neuropsychopharmacology* **41**, 906–915 (2016).
17. R. C. Twining *et al.*, Aversive stimuli drive drug seeking in a state of low dopamine tone. *Biol. Psychiatry* **77**, 895–902 (2015).
18. A. G. DiFeliceantonio, K. C. Berridge, Dorsolateral neostriatum contribution to incentive salience: Opioid or dopamine stimulation makes one reward cue more motivationally attractive than another. *Eur. J. Neurosci.* **43**, 1203–1218 (2016).
19. K. C. Berridge, T. E. Robinson, Liking, wanting, and the incentive-sensitization theory of addiction. *Am. Psychol.* **71**, 670–679 (2016).
20. J. D. Salamone *et al.*, Mesolimbic dopamine and the regulation of motivated behavior. *Curr. Top. Behav. Neurosci.* **27**, 231–257 (2016).
21. K. C. Berridge, From prediction error to incentive salience: Mesolimbic computation of reward motivation. *Eur. J. Neurosci.* **35**, 1124–1143 (2012).
22. T. E. Robinson, K. C. Berridge, The neural basis of drug craving: An incentive-sensitization theory of addiction. *Brain Res. Brain Res. Rev.* **18**, 247–291 (1993).
23. J. F. Cheer *et al.*, Coordinated accumbal dopamine release and neural activity drive goal-directed behavior. *Neuron* **54**, 237–244 (2007).
24. L. T. Coddington, J. T. Dudman, The timing of action determines reward prediction signals in identified midbrain dopamine neurons. *Nat. Neurosci.* **21**, 1563–1573 (2018).

25. L. T. Coddington, J. T. Dudman, Learning from action: Reconsidering movement signaling in midbrain dopamine neuron activity. *Neuron* **104**, 63–77 (2019).
26. I. B. Witten *et al*., Recombinase-driver rat lines: Tools, techniques, and optogenetic application to dopamine-mediated reinforcement. *Neuron* **72**, 721–733 (2011).
27. C. Wilson, G. G. Nomikos, M. Collu, H. C. Fibiger, Dopaminergic correlates of motivated behavior: Importance of drive. *J. Neurosci.* **15**, 5169–5178 (1995).
28. J. J. Cone, J. E. McCutcheon, M. F. Roitman, Ghrelin acts as an interface between physiological state and phasic dopamine signaling. *J. Neurosci.* **34**, 4905–4913 (2014).
29. S. Y. Branch *et al*., Food restriction increases glutamate receptor-mediated burst firing of dopamine neurons. *J. Neurosci.* **33**, 13861–13872 (2013).
30. V. R. Konanur, T. M. Hsu, S. E. Kanoski, M. R. Hayes, M. F. Roitman, Phasic dopamine responses to a food-predictive cue are suppressed by the glucagon-like peptide-1 receptor agonist Exendin-4. *Physiol. Behav.* **215**, 112771 (2020).
31. S. M. Fortin, M. F. Roitman, Challenges to body fluid homeostasis differentially recruit phasic dopamine signaling in a taste-selective manner. *J. Neurosci.* **38**, 6841–6853 (2018).
32. J. J. Cone *et al*., Physiological state gates acquisition and expression of mesolimbic reward prediction signals. *Proc. Natl. Acad. Sci. U.S.A.* **113**, 1943–1948 (2016).
33. H. Lütcke *et al*., Optical recording of neuronal activity with a genetically-encoded calcium indicator in anesthetized and freely moving mice. *Front. Neural Circuits* **4**, 9 (2010).
34. T. Patriarchi *et al*., Ultrafast neuronal imaging of dopamine dynamics with designed genetically encoded sensors. *Science* **360**, eaat4422 (2018).
35. J. W. de Jong *et al*., A neural circuit mechanism for encoding aversive stimuli in the mesolimbic dopamine system. *Neuron* **101**, 133–151.e7 (2019).
36. M. Morales, E. B. Margolis, Ventral tegmental area: Cellular heterogeneity, connectivity and behaviour. *Nat. Rev. Neurosci.* **18**, 73–85 (2017).
37. S. Lammel *et al*., Input-specific control of reward and aversion in the ventral tegmental area. *Nature* **491**, 212–217 (2012).
38. S. Lammel *et al*., Diversity of transgenic mouse models for selective targeting of midbrain dopamine neurons. *Neuron* **85**, 429–438 (2015).
39. A. Lak, W. R. Stauffer, W. Schultz, Dopamine prediction error responses integrate subjective value from different reward dimensions. *Proc. Natl. Acad. Sci. U.S.A.* **111**, 2343–2348 (2014).
40. W. Schultz, P. Dayan, P. R. Montague, A neural substrate of prediction and reward. *Science* **275**, 1593–1599 (1997).
41. J. J. Day, M. F. Roitman, R. M. Wightman, R. M. Carelli, Associative learning mediates dynamic shifts in dopamine signaling in the nucleus accumbens. *Nat. Neurosci.* **10**, 1020–1028 (2007).
42. M. F. Roitman, G. D. Stuber, P. E. Phillips, R. M. Wightman, R. M. Carelli, Dopamine operates as a subsecond modulator of food seeking. *J. Neurosci.* **24**, 1265–1271 (2004).
43. G. D. Stuber *et al*., Reward-predictive cues enhance excitatory synaptic strength onto midbrain dopamine neurons. *Science* **321**, 1690–1692 (2008).
44. J. D. Berke, What does dopamine mean? *Nat. Neurosci.* **21**, 787–793 (2018).
45. M. Tschöp, D. L. Smiley, M. L. Heiman, Ghrelin induces adiposity in rodents. *Nature* **407**, 908–913 (2000).
46. D. L. Drazen, T. P. Vahl, D. A. D'Alessio, R. J. Seeley, S. C. Woods, Effects of a fixed meal pattern on ghrelin secretion: Evidence for a learned response independent of nutrient status. *Endocrinology* **147**, 23–30 (2006).
47. D. E. Cummings *et al*., A preprandial rise in plasma ghrelin levels suggests a role in meal initiation in humans. *Diabetes* **50**, 1714–1719 (2001).
48. M. Nakazato *et al*., A role for ghrelin in the central regulation of feeding. *Nature* **409**, 194–198 (2001).
49. D. Daniels, D. K. Yee, L. F. Faulconbridge, S. J. Fluharty, Divergent behavioral roles of angiotensin receptor intracellular signaling cascades. *Endocrinology* **146**, 5552–5560 (2005).
50. S. Morita, S. Miyata, Different vascular permeability between the sensory and secretory circumventricular organs of adult mouse brain. *Cell Tissue Res.* **349**, 589–603 (2012).
51. R. W. Lind, L. W. Swanson, D. Ganten, Angiotensin II immunoreactivity in the neural afferents and efferents of the subfornical organ of the rat. *Brain Res.* **321**, 209–215 (1984).
52. W. Schultz, Reward signaling by dopamine neurons. *Neuroscientist* **7**, 293–302 (2001).
53. A. A. Hamid *et al*., Mesolimbic dopamine signals the value of work. *Nat. Neurosci.* **19**, 117–126 (2016).
54. B. Engelhard *et al*., Specialized coding of sensory, motor and cognitive variables in VTA dopamine neurons. *Nature* **570**, 509–513 (2019).
55. C. J. Burnett *et al*., Hunger-driven motivational state competition. *Neuron* **92**, 187–201 (2016).
56. W. H. Shyu *et al*., Neural circuits for long-term water-reward memory processing in thirsty Drosophila. *Nat. Commun.* **8**, 15230 (2017).
57. B. Senapati *et al*., A neural mechanism for deprivation state-specific expression of relevant memories in Drosophila. *Nat. Neurosci.* **22**, 2029–2039 (2019).
58. V. Augustine *et al*., Temporally and spatially distinct thirst satiation signals. *Neuron* **103**, 242–249.e4 (2019).
59. B. G. Hoebel, P. Rada, G. P. Mark, L. Hernandez, The power of integrative peptides to reinforce behavior by releasing dopamine. *Ann. N. Y. Acad. Sci.* **739**, 36–41 (1994).
60. I. Merchenthaler, M. Lane, P. Shughrue, Distribution of pre-pro-glucagon and glucagon-like peptide-1 receptor messenger RNAs in the rat central nervous system. *J. Comp. Neurol.* **403**, 261–280 (1999).
61. J. D. Hommel *et al*., Leptin receptor signaling in midbrain dopamine neurons regulates feeding. *Neuron* **51**, 801–810 (2006).
62. J. M. Zigman, J. E. Jones, C. E. Lee, C. B. Saper, J. K. Elmquist, Expression of ghrelin receptor mRNA in the rat and the mouse brain. *J. Comp. Neurol.* **494**, 528–548 (2006).
63. P. M. Sexton, G. Paxinos, M. A. Kenney, P. J. Wookey, K. Beaumont, In vitro autoradiographic localization of amylin binding sites in rat brain. *Neuroscience* **62**, 553–567 (1994).
64. M. M. Scott *et al*., Leptin targets in the mouse brain. *J. Comp. Neurol.* **514**, 518–532 (2009).
65. S. C. Cork *et al*., Distribution and characterisation of Glucagon-like peptide-1 receptor expressing cells in the mouse brain. *Mol. Metab.* **4**, 718–731 (2015).
66. J. L. Marks, D. Porte Jr, W. L. Stahl, D. G. Baskin, Localization of insulin receptor mRNA in rat brain by in situ hybridization. *Endocrinology* **127**, 3234–3236 (1990).
67. S. Liu, S. L. Borgland, Regulation of the mesolimbic dopamine circuit by feeding peptides. *Neuroscience* **289**, 19–42 (2015).
68. Z. Lenkei, M. Palkovits, P. Corvol, C. Llorens-Cortes, Distribution of angiotensin type-1 receptor messenger RNA expression in the adult rat brain. *Neuroscience* **82**, 827–841 (1998).
69. T. M. Hsu, J. E. McCutcheon, M. F. Roitman, Parallels and overlap: The integration of homeostatic signals by mesolimbic dopamine neurons. *Front. Psychiatry* **9**, 410 (2018).
70. M. A. Rossi, G. D. Stuber, Overlapping brain circuits for homeostatic and hedonic feeding. *Cell Metab.* **27**, 42–56 (2018).
71. C. M. Liu, S. E. Kanoski, Homeostatic and non-homeostatic controls of feeding behavior: Distinct vs. common neural systems. *Physiol. Behav.* **193**, 223–231 (2018).
72. V. Augustine *et al*., Hierarchical neural architecture underlying thirst regulation. *Nature* **555**, 204–209 (2018).
73. D. E. Leib *et al*., The forebrain thirst circuit drives drinking through negative reinforcement. *Neuron* **96**, 1272–1281.e4 (2017).
74. R. R. Miselis, The efferent projections of the subfornical organ of the rat: A circumventricular organ within a neural network subserving water balance. *Brain Res.* **230**, 1–23 (1981).
75. L. W. Swanson, R. W. Lind, Neural projections subserving the initiation of a specific motivated behavior in the rat: New projections from the subfornical organ. *Brain Res.* **379**, 399–403 (1986).
76. G. Kurt, H. L. Woodworth, S. Fowler, R. Bugescu, G. M. Leinninger, Activation of lateral hypothalamic area neurotensin-expressing neurons promotes drinking. *Neuropharmacology* **154**, 13–21 (2019).
77. J. A. Brown *et al*., Distinct subsets of lateral hypothalamic neurotensin neurons are activated by leptin or dehydration. *Sci. Rep.* **9**, 1873 (2019).
78. S. W. Hurley, H. A. Arseth, A. K. Johnson, Orexin neurons couple neural systems mediating fluid balance with motivation-related circuits. *Behav. Neurosci.* **132**, 284–292 (2018).
79. T. S. Thomas, C. Baimel, S. L. Borgland, Opioid and hypocretin neuromodulation of ventral tegmental area neuronal subpopulations. *Br. J. Pharmacol.* **175**, 2825–2833 (2018).
80. J. N. Betley *et al*., Neurons for hunger and thirst transmit a negative-valence teaching signal. *Nature* **521**, 180–185 (2015).
81. Y. Chen, Y. C. Lin, C. A. Zimmerman, R. A. Essner, Z. A. Knight, Hunger neurons drive feeding through a sustained, positive reinforcement signal. *eLife* **5**, e18640 (2016).
82. National Research Council, *Guide for the Care and Use of Laboratory Animals* (National Academies Press, Washington, DC, ed. 8, 2011).